Machine Learning predicts laboratory earthquakes

Bertrand Rouet-Leduc[1,2], Claudia Hulbert[1], Nicholas Lubbers[1,3], Kipton Barros[1], Colin Humphreys[2], Paul A. Johnson[4]

Bertrand Rouet-Leduc, bertrandrl@lanl.gov

[1]Los Alamos National Laboratory, Theoretical Division and CNLS, Los Alamos, New Mexico.

[2]University of Cambridge, Department of Materials Science and Metallurgy, Cambridge CB3 0FS, UK.

[3]Boston University, Department of Physics, Boston Massachusetts.

[4]Los Alamos National Laboratory, Geophysics Group, Los Alamos, New Mexico.

This article has been accepted for publication and undergone full peer review but has not been through the copyediting, typesetting, pagination and proofreading process, which may lead to differences between this version and the Version of Record. Please cite this article as doi: 10.1002/2017GL074677

Abstract. We apply machine learning to data sets from shear laboratory experiments, with the goal of identifying hidden signals that precede earthquakes. Here we show that by listening to the acoustic signal emitted by a laboratory fault, machine learning can predict the time remaining before it fails with great accuracy. These predictions are based solely on the instantaneous physical characteristics of the acoustical signal, and do not make use of its history. Surprisingly, machine learning identifies a signal emitted from the fault zone previously thought to be low-amplitude noise that enables failure forecasting throughout the laboratory quake cycle. We infer that this signal originates from continuous grain motions of the fault gouge as the fault blocks displace. We posit that applying this approach to continuous seismic data may lead to significant advances in identifying currently unknown signals, in providing new insights into fault physics, and in placing bounds on fault failure times.

Keypoints:

- Machine learning appears to discern the frictional state when applied to laboratory seismic data recorded during a shear experiment
- Machine learning uses statistical characteristics of the recorded seismic signal to accurately predict slip failure time
- The work has import to identifying new geophysical signals of all kinds and potentially to earthquake forecasting, and is applicable to potentially

all failure scenarios including brittle failure, avalanche, landslide, volcanic eruption etc.

1. Introduction

A classical approach to determining that an earthquake may be looming is based on the inter-event time (recurrence interval) for characteristic earthquakes, earthquakes that repeat periodically [*Schwartz and Coppersmith* [1984]]. For instance, analysis of turbidite stratigraphy deposited during successive earthquakes dating back 10,000 years suggests the Cascadia subduction zone is ripe for a megaquake [*Goldfinger et al.* [2017]]. The idea behind characteristic, repeating earthquakes was the basis of the well-known Parkfield prediction based strictly on seismic data. Similar earthquakes occurring between 1857 and 1966 suggested a recurrence interval of 21.9±3.1 years and thus an earthquake was expected between 1988-1993 [*Bakun and Lindh* [1985]], but ultimately took place in 2004. With this approach, as earthquake recurrence is not constant for a given fault, event occurrence can only be inferred within large error bounds. Over the last 15 years, there has been renewed hope that progress can be made regarding forecasting owing to tremendous advances in instrumentation quality and density. These advances have led to exciting discoveries of previously unidentified slip processes that include slow slip [*Melbourne and Webb* [2003]], Low Frequency Earthquakes and Earth tremor [*Shelly et al.* [2007]; *Obara* [2002]; *Brown et al.* [2009]] that occur deep in faults. These discoveries inform a new understanding of fault slip and may well lead to advances in forecasting impending fault failure if the coupling of deep faults to the seismogenic zone can be unraveled. The advances in instrumentation sensitivity and density also provide new means to record small events that may be precursors. Acoustic/seismic precursors to failure appear to be a nearly universal phenomenon in materials. For instance, it is well established that

failure in granular materials [*Michlmayr et al.* [2013]] and in avalanche [*Pradhan et al.* [2006]] is frequently accompanied by impulsive acoustic/seismic precursors, many of them very small. Precursors are also routinely observed in brittle failure of a spectrum of industrial [*Huang et al.* [1998]] and Earth materials [*Schubnel et al.* [2013]; *Jaeger et al.* [2007]]. Precursors are observed in laboratory faults [*Johnson et al.* [2013]; *W. Goebel et al.* [2013]] and are widely but not systematically observed preceding earthquakes [*Bouchon et al.* [2013, 2016]; *McGuire et al.* [2015]; *Mignan* [2014]; *Wyss and Booth* [1997]; *Geller* [1997]]. Seismic swarm activity which exhibits very different statistical characteristics than classical impulsive precursors may or may not precede large earthquakes but can mask classical precursors (e.g., *Ishibashi* [1988]). The International Commission on Earthquake Forecasting for Civil Protection concluded in 2011 there was "considerable room for methodological improvements in this type of [precursor-based failure forecasting] research" [International Commission on Earthquake Forecasting for Civil Protection, 2011: *Jordan et al.* [2011]]. The commission also concluded that published results may be biased toward positive observations. We hypothesize that precursors are a manifestation of critical stress conditions preceding shear failure. We posit that seismic precursor magnitudes can be very small and thus frequently go unrecorded or unidentified. As instrumentation improves, precursors may ultimately be found to exist for most or all earthquakes [*Delorey et al.* [2017]]. Furthermore, it is plausible that other signals exist that presage failure.

2. Materials and Methods

Here we apply recent advances in machine learning to data from a well characterized laboratory system [*Johnson et al.* [2013]; *Marone* [1998]; *Niemeijer et al.* [2010]; *Scuderi*

et al. [2014]]. Our laboratory system is a two-fault configuration that contains fault gouge material submitted to double direct shear (see text S1, Fig. S1). The driving piston displaces at a very constant velocity of 5 microns/sec during the inter-event time, and accelerates briefly during slip with a calibrated accuracy of 0.1 micron/sec. An accelerometer records the acoustic emission (AE) emanating from the shearing layers. The shear stress imposed by the driving block is also monitored (Figs. 1, 2a, S1), as well as other physical parameters such as the shearing rate, gouge layer thickness, friction and the applied load [*Johnson et al.* [2013]; *Marone* [1998]; *Niemeijer et al.* [2010]]. The steel blocks are extremely stiff (order 160 GPa) so the deformation takes place largely in the gouge. Following a stick-slip frictional failure (laboratory earthquake), the shearing block displaces while the gouge material simultaneously dilates and strengthens, as manifested by increasing shear stress (Figs. 1a, S1) and friction. As the material approaches failure, it exhibits characteristics of a critical stress regime, including many small shear failures that emit impulsive AEs [*Johnson et al.* [2013]]. This unstable state concludes with a laboratory earthquake, in which the shearing block rapidly displaces, the friction and shear stress decrease precipitously due to the gouge failure (Fig. S1, top), and the gouge layers simultaneously compact. Under a broad range of load and shear velocity conditions, the apparatus stick-slips quasi-periodically for hundreds of stress cycles during a single experiment [*Marone* [1998]; *Niemeijer et al.* [2010]], and in general follows predictions from rate and state friction [e.g., *Marone* [1998]]. The rate of impulsive precursors accelerates as failure approaches [*Johnson et al.* [2013]], suggesting that upcoming laboratory earthquake timing could be predicted. In this work, we ask: can the failure time of an upcoming

laboratory earthquake be predicted using characteristics of only the continuously recorded acoustic signal?

Our goal is to predict the time remaining before the next failure (Fig. 1a, bottom) using only local, moving time windows of the AE data (Fig. 1b, top). We apply a machine learning technique, the random forest (RF) [*Breiman* [2001]; *Pedregosa et al.* [2011]; *Louppe et al.* [2013]], to the continuous acoustic time series data recorded from the fault (see Fig. 1 and text S2, S3). The RF model is an average over a set of decision trees (Fig. 1c). Each decision tree predicts the time remaining before the next failure using a sequence of decisions based on statistical features derived from the time windows. Figure 1a, top, shows the laboratory shear stress exhibiting multiple failure events during an experiment.

From each time window, we compute a set of approximately 100 potentially relevant statistical features (e.g. mean, variance, kurtosis, autocorrelation, etc.). The most useful features are then selected recursively [*Gregorutti et al.* [2017]]. The RF uses these selected features to predict the time remaining before the next failure (text S4). Fig. 1b shows four of these features on the same time scale as in Fig. 1a, through multiple failure cycles. Some features are sensitive to changes in signal characteristics early in time during the stress cycle, just following a laboratory earthquake. All features shown are strongly sensitive to signal characteristics just preceding failure, as the system approaches shear-stress criticality.

3. Results

Fig. 1d and 2 show failure predictions on testing data-the acoustic signal corresponding to a sequence of slip events the model has never seen. We emphasize that there is no past

or future information considered when making a prediction (blue curve): each prediction uses only the information within one single time window of the acoustic signal. Thus, by listening to the acoustic signal currently emitted by the system, we predict the time remaining before it fails-a 'now' prediction based on the instantaneous physical characteristics of the system that does not make use of its history. We quantify the accuracy of our model using R2, the coefficient of determination.

A naïve model based exclusively on the periodicity of the events (average inter-event time) only achieves an R2 performance of 0.3 (See Fig. S2). In comparison, the time to failure predictions from the RF model are highly accurate, with an R2 value of 0.89. Surprisingly, the RF model accurately predicts failure not only when failure is imminent, but throughout the entire laboratory earthquake cycle, demonstrating that the system continuously progresses towards failure. This is unexpected, as impulsive precursors are only observed while the system is in a critical stress state. We find that statistics quantifying the signal amplitude distribution (e.g. its variance and higher order moments) are highly effective at forecasting failure. The variance, which characterizes overall signal amplitude fluctuation, is the strongest single feature early in time (Fig. 1b). As the system nears failure, other outlier statistics such as the kurtosis and thresholds become predictive as well. These outlier statistics are responding to the impulsive precursor AE (Fig. 3c) typically observed as a material approaches failure [*Huang et al.* [1998]], including those under shear conditions in the laboratory [*Johnson et al.* [2013]] and in Earth [*Bouchon et al.* [2013, 2016]; *Wyss and Booth* [1997]]. These signals are due to small, observable shear failures within the gouge immediately preceding the laboratory earthquake [*Johnson et al.* [2013]].

Our machine learning analysis provides new insight into the slip physics. Specifically, the AE signal occurring long before failure was previously assumed to be noise and thus overlooked, illustrating human bias that ML can overcome [*Johnson et al.* [2013]]. This signal bears resemblance to non-volcanic tremor [*Shelly et al.* [2007]; *Obara* [2002]; *Brown et al.* [2009]] associated with slow slip [*Rogers and Dragert* [2003]; *Rubinstein et al.* [2009]], that exhibits ringing characteristics over long periods of time. An important difference is that tremor is isolated in time. In the laboratory experiments, the central block (Fig. S1) slowly slips throughout the stress cycle, briefly accelerating at the time of failure. Fig. (3b) shows a raw time series far from failure. The signal exhibits small modulations that are challenging to identify by eye and persist throughout the stress cycle. These modulations increase in amplitude as failure is approached, as measured by the increase in signal variance. This increase in signal variance shows that the energy carried by the acoustic signal steadily increases throughout the stress cycle. We posit that these variations are due to systematic groaning, creaking and chattering from continuous grain motions of the fault gouge due to slow slipping of the block (Discrete Element Modeling of this system [*Ferdowsi et al.* [2014]; *Dorostkar et al.*, 2017]] is ongoing to further investigate the origin of this new found signal). Our ML-driven analysis suggests that the system emits a small but progressively increasing amount of energy throughout the stress cycle, before abruptly releasing the accumulated energy when a slip event takes place (Figs. S3, S4). The predictions of our model generalize across experimental conditions. To demonstrate this, we trained the system at one applied load level, and then tested it on data from different load levels, exhibiting different inter-event times between failures. We observe that the model predictions retain their accuracy across load levels and correctly predicts

clear outliers (see Fig. S5). The fact that timing prediction can be made under conditions the RF has never seen suggests that the time series signal is capturing fundamental physics that lead to the prediction. Further, when the stress-cycle periodicity is disrupted by a shorter recurrence time as shown in the inset of Fig. 2, the RF still does an excellent job in predicting failure time, showing that the approach can be generalized to aperiodic fault cycles. The fact that timing prediction can be made under conditions the RF has never seen suggests that the time series signal is capturing fundamental physics that lead to the prediction. Our physical interpretation is that the chattering signal variance and higher order moments are a fingerprint of the instantaneous friction and shear-stress state, the variance and other features of the time series carry quantitative frictional state information (see Figs. S3-S4), informing the RF of when the next slip event will occur. If true, this is a remarkable observation in itself. We are currently working on the relation between the signal variance and friction to determine if indeed there is a direct link.

There are a number of issues to consider in applying what we have learned to Earth. The laboratory shear rates are orders of magnitude larger than Earth (5 microns/sec vs mms-cms/year). The laboratory temperature conditions in no way resemble those in Earth, while the pressures could be representative of in situ pressures when fluid pressures are large. While it is a significant leap linking the laboratory studies to Earth scale, we know from past work [*Johnson et al.* [2013]; *W. Goebel et al.* [2013]] that the fundamental scaling relation in fault physics, the Gutenberg-Richter relation calculated from the laboratory precursors [*Gutenberg and Richter* [1949]], is within the bounds observed in Earth [*Johnson et al.* [2013]; *W. Goebel et al.* [2013]]. This similarity implies that some of the important fault frictional physics scale. A laboratory experiment clearly cannot capture

all of the physics of a complex rupture in Earth. Nevertheless, the machine learning expertise we are developing as we move from the laboratory to Earth will ultimately guide further work at large scale.

4. Conclusion

To summarize, we show that ML applied to this experiment provides accurate failure forecasts based on the instantaneous analysis of the acoustic signal at any time in the slip cycle, and reveals a signal previously unidentified. These results should suffice to encourage ML analysis of seismic signals in Earth. To our knowledge, this is the first application of ML to continuous acoustic/seismic data with the goal of inferring failure times. These results suggest that previous analyses based exclusively on earthquake catalogs [*Keilis-Borok et al.* [1988]; *Liu et al.* [2005]; *Alves* [2006]; *Alexandridis et al.* [2014]] may be incomplete. In particular, ML-based approaches mitigate human bias by automatically searching for patterns in a large space of potentially relevant variables. Our current approach is to progressively scale from the laboratory to the Earth by applying this approach to Earth problems that most resemble the laboratory system. An interesting analogy to the laboratory may be faults that exhibit small repeating earthquakes. For instance, fault patches located on the San Andreas Fault near Parkfield [*Nadeau and McEvilly* [1999]; *Zechar and Nadeau* [2012]] exhibit such behavior. Repeaters at these fault patches may be emitting chattering in analogy to the laboratory. If so, can this signal be recorded by borehole and surface instruments? We are currently studying this problem. Whether ML approaches applied to continuous seismic or other geophysical data succeed in providing information on timing of earthquakes (not to mention the challenge of predicting earthquake magnitude), this approach may reveal unidentified signals

associated with undiscovered fault physics. Furthermore, this method may be useful for failure prediction in a broad spectrum of industrial and natural materials. Technology is at a confluence of dramatic advances in instrumentation, machine learning, the ability to handle massive data sets and faster computers. Thus, the stage has been set for potentially marked advances in earthquake science.

Acknowledgments

We acknowledge funding from Institutional Support (LDRD) at Los Alamos National Laboratory including funding via the Center for Nonlinear Studies. We thank Chris Marone for access to, and help with, experiments, and comments to the manuscript. We thank Andrew Delorey, Thorne Lay, Christopher Ren, Barbara Romanowicz, Chris Scholz and Bill Ellsworth for helpful comments and/or discussions. We thank Jamal Mohd-Yusof for suggesting applying machine learning to this data set. All the data used is freely available on the data repository hosted Prof. Chris Marone at the Pennsylvania State University.

References

Alexandridis, A., E. Chondrodima, E. Efthimiou, G. Papadakis, F. Vallianatos, and D. Triantis (2014), Large earthquake occurrence estimation based on radial basis function neural networks, *IEEE Transactions on Geoscience and Remote Sensing*, *52*(9), 5443–5453, doi:10.1109/TGRS.2013.2288979.

Alves, E. I. (2006), Earthquake forecasting using neural networks: Results and future work, *Nonlinear Dynamics*, *44*(1), 341–349, doi:10.1007/s11071-006-2018-1.

Bakun, W. H., and A. G. Lindh (1985), The Parkfield, California, Earthquake Prediction Experiment, *Science*, *229*, 619–624, doi:10.1126/science.229.4714.619.

Bouchon, M., V. Durand, D. Marsan, H. Karabulut, and J. Schmittbuhl (2013), The long precursory phase of most large interplate earthquakes, *Nature geoscience*, *6*(4), 299.

Bouchon, M., D. Marsan, V. Durand, M. Campillo, H. Perfettini, R. Madariaga, and B. Gardonio (2016), Potential slab deformation and plunge prior to the tohoku, iquique and maule earthquakes, *Nature Geoscience*, *9*(5), 380–383.

Breiman, L. (2001), Random forests, *Machine Learning*, *45*(1), 5–32, doi:10.1023/A:1010933404324.

Brown, J. R., G. C. Beroza, S. Ide, K. Ohta, D. R. Shelly, S. Y. Schwartz, W. Rabbel, M. Thorwart, and H. Kao (2009), Deep low-frequency earthquakes in tremor localize to the plate interface in multiple subduction zones, *Geophysical Research Letters*, *36*(19).

Delorey, A. A., N. J. van der Elst, and P. A. Johnson (2017), Tidal triggering of earthquakes suggests poroelastic behavior on the san andreas fault, *Earth and Planetary Science Letters*, *460*, 164 – 170, doi:https://doi.org/10.1016/j.epsl.2016.12.014.

Dorostkar, O., R. A. Guyer, P. A. Johnson, C. Marone, and J. Carmeliet (), On the micromechanics of slip events in sheared, fluid saturated fault gouge, *Geophysical Research Letters*.

Dorostkar, O., R. A. Guyer, P. A. Johnson, C. Marone, and J. Carmeliet (2017), On the role of fluids in stick-slip dynamics of saturated granular fault gouge using a coupled computational fluid dynamics-discrete element approach, *Journal of Geophysical Research: Solid Earth*, *122*(5), 3689–3700, doi:10.1002/2017JB014099, 2017JB014099.

Ferdowsi, B., M. Griffa, R. A. Guyer, P. A. Johnson, C. Marone, and J. Carmeliet (2014), Three-dimensional discrete element modeling of triggered slip in sheared granular media, *Phys. Rev. E*, *89*, 042,204, doi:10.1103/PhysRevE.89.042204.

Geller, R. J. (1997), Earthquake prediction: a critical review, *Geophysical Journal International*, *131*(3), 425–450, doi:10.1111/j.1365-246X.1997.tb06588.x.

Goldfinger, C., S. Galer, J. Beeson, T. Hamilton, B. Black, C. Romsos, J. Patton, C. H. Nelson, R. Hausmann, and A. Morey (2017), The importance of site selection, sediment supply, and hydrodynamics: A case study of submarine paleoseismology on the northern cascadia margin, washington usa, *Marine Geology*, *384*, 4 – 46, doi:http://dx.doi.org/10.1016/j.margeo.2016.06.008, subaquatic paleoseismology: records of large Holocene earthquakes in marine and lacustrine sediments.

Gregorutti, B., B. Michel, and P. Saint-Pierre (2017), Correlation and variable importance in random forests, *Statistics and Computing*, *27*(3), 659–678.

Gutenberg, B., and C. F. Richter (1949), *Seismicity of the Earth,*, Princeton University Press, Princeton, NJ.

Huang, M., L. Jiang, P. K. Liaw, C. R. Brooks, R. Seeley, and D. L. Klarstrom (1998), Using acoustic emission in fatigue and fracture materials research, *JOM*, *50*(11), 1–14.

Ishibashi, K. (1988), Two categories of earthquake precursors, physical and tectonic, and their roles in intermediate-term earthquake prediction, *Pure and Applied Geophysics*, *126*(2), 687–700.

Jaeger, J., N. Cook, and R. Zimmerman (2007), *Poroelasticity and thermoelasticity*, 168–204 pp.

Johnson, P. A., B. Ferdowsi, B. M. Kaproth, M. Scuderi, M. Griffa, J. Carmeliet, R. A. Guyer, P.-Y. Le Bas, D. T. Trugman, and C. Marone (2013), Acoustic emission and microslip precursors to stick-slip failure in sheared granular material, *Geophysical Research Letters*, *40*(21), 5627–5631, doi:10.1002/2013GL057848, 2013GL057848.

Jordan, T., Y.-T. Chen, P. Gasparini, R. Madariaga, I. Main, W. Marzocchi, G. Papadopoulos, G. Sobolev, K. Yamaoka, and J. Zschau (2011), Operational earthquake forecasting. state of knowledge and guidelines for utilization, *Annals of Geophysics*, *54*(4), doi:10.4401/ag-5350.

Keilis-Borok, V., L. Knopoff, I. Rotwain, and C. Allen (1988), Intermediate-term prediction of occurrence times of strong earthquakes, *Nature*, *335*(6192), 690–694.

Liu, Y., Y. Li, G. Li, B. Zhang, and G. Wu (2005), Constructive ensemble of rbf neural networks and its application to earthquake prediction, *Advances in Neural Networks*, pp. 532–537.

Louppe, G., L. Wehenkel, A. Sutera, and P. Geurts (2013), Understanding variable importances in forests of randomized trees, pp. 431–439.

Marone, C. (1998), Laboratory-derived friction laws and their application to seismic faulting, *Annual Review of Earth and Planetary Sciences*, *26*(1), 643–696.

McGuire, J. J., R. B. Lohman, R. D. Catchings, M. J. Rymer, and M. R. Goldman (2015), Relationships among seismic velocity, metamorphism, and seismic and aseismic fault slip in the salton sea geothermal field region, *Journal of Geophysical Research: Solid Earth*, *120*(4), 2600–2615, doi:10.1002/2014JB011579, 2014JB011579.

Melbourne, T. I., and F. H. Webb (2003), Slow but not quite silent, *Science*, *300*(5627), 1886–1887, doi:10.1126/science.1086163.

Michlmayr, G., D. Cohen, and D. Or (2013), Shear-induced force fluctuations and acoustic emissions in granular material, *Journal of Geophysical Research: Solid Earth*, *118*(12), 6086–6098, doi:10.1002/2012JB009987.

Mignan, A. (2014), The debate on the prognostic value of earthquake foreshocks: A meta-analysis, *Scientific reports*, *4*.

Nadeau, R. M., and T. V. McEvilly (1999), Fault slip rates at depth from recurrence intervals of repeating microearthquakes, *Science*, *285*(5428), 718–721, doi:10.1126/science.285.5428.718.

Niemeijer, A., C. Marone, and D. Elsworth (2010), Frictional strength and strain weakening in simulated fault gouge: Competition between geometrical weakening and chemical strengthening, *Journal of Geophysical Research: Solid Earth*, *115*(B10), n/a–n/a, doi:10.1029/2009JB000838, b10207.

Obara, K. (2002), Nonvolcanic deep tremor associated with subduction in southwest japan, *Science*, *296*(5573), 1679–1681, doi:10.1126/science.1070378.

Pedregosa, F., G. Varoquaux, A. Gramfort, V. Michel, B. Thirion, O. Grisel, M. Blondel, P. Prettenhofer, R. Weiss, V. Dubourg, et al. (2011), Scikit-learn: Machine learning in python, *Journal of Machine Learning Research*, *12*(Oct), 2825–2830.

Pradhan, S., A. Hansen, and P. C. Hemmer (2006), Crossover behavior in failure avalanches, *Phys. Rev. E*, *74*, 016,122, doi:10.1103/PhysRevE.74.016122.

Rogers, G., and H. Dragert (2003), Episodic tremor and slip on the cascadia subduction zone: The chatter of silent slip, *Science*, *300*(5627), 1942–1943, doi:10.1126/science.1084783.

Rubinstein, J. L., D. R. Shelly, and W. L. Ellsworth (2009), Non-volcanic tremor: A window into the roots of fault zones, in *New Frontiers in Integrated Solid Earth Sciences*, pp. 287–314, Springer.

Schubnel, A., F. Brunet, N. Hilairet, J. Gasc, Y. Wang, and H. W. Green (2013), Deep-focus earthquake analogs recorded at high pressure and temperature in the laboratory, *Science*, *341*(6152), 1377–1380, doi:10.1126/science.1240206.

Schwartz, D. P., and K. J. Coppersmith (1984), Fault behavior and characteristic earthquakes: Examples from the wasatch and san andreas fault zones, *Journal of Geophysical Research: Solid Earth*, *89*(B7), 5681–5698, doi:10.1029/JB089iB07p05681.

Scuderi, M. M., B. M. Carpenter, and C. Marone (2014), Physicochemical processes of frictional healing: Effects of water on stick-slip stress drop and friction of granular fault gouge, *Journal of Geophysical Research: Solid Earth*, *119*(5), 4090–4105, doi:10.1002/2013JB010641, 2013JB010641.

Shelly, D. R., G. C. Beroza, and S. Ide (2007), Non-volcanic tremor and low-frequency earthquake swarms, *Nature*, *446*(7133), 305.

W. Goebel, T. H., D. Schorlemmer, T. W. Becker, G. Dresen, and C. G. Sammis (2013), Acoustic emissions document stress changes over many seismic cycles in stick-slip experiments, *Geophysical Research Letters*, *40*(10), 2049–2054, doi:10.1002/grl.50507.

Wyss, M., and D. C. Booth (1997), The iaspei procedure for the evaluation of earthquake precursors, *Geophysical Journal International*, *131*(3), 423–424.

Zechar, J. D., and R. M. Nadeau (2012), Predictability of repeating earthquakes near parkfield, california, *Geophysical Journal International*, *190*(1), 457–462.

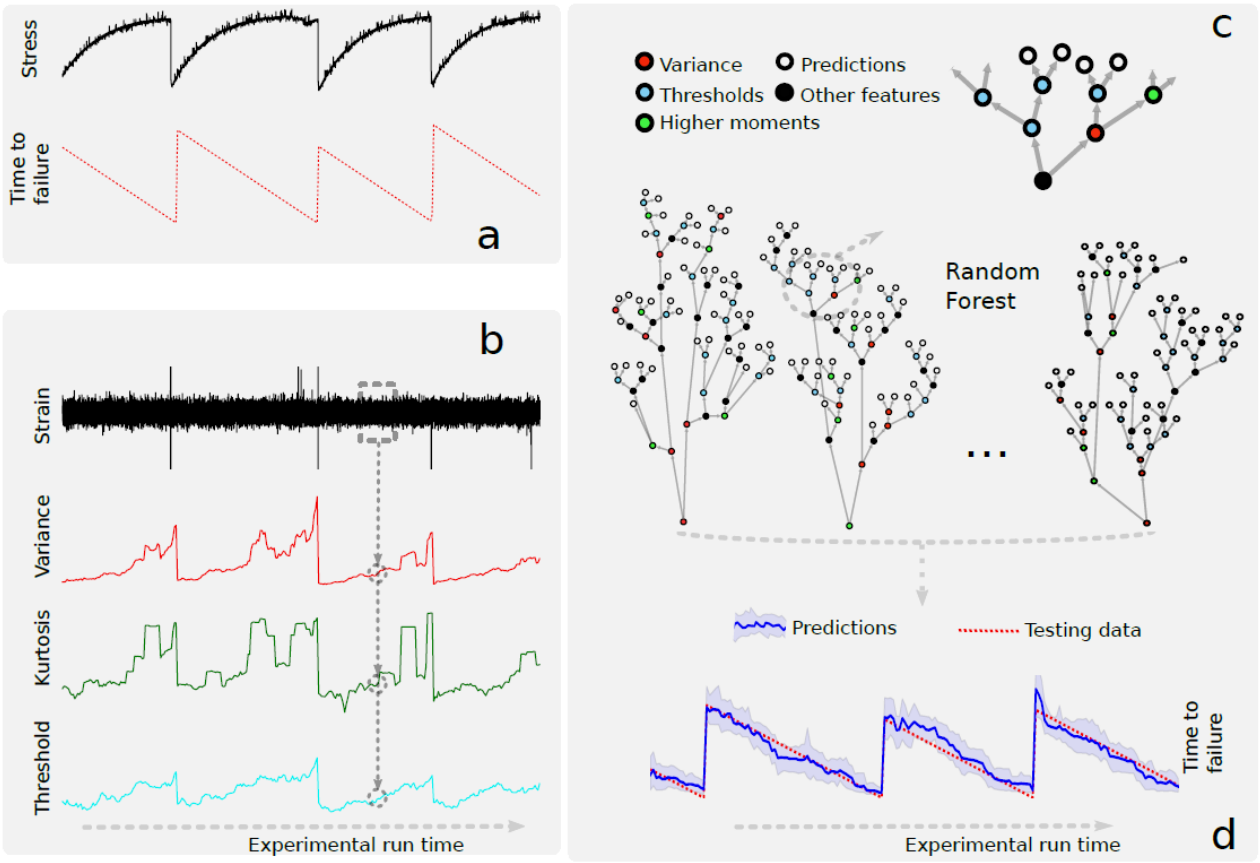

Figure 1. Random Forest (RF) approach for predicting time remaining before failure. (a) Shear stress (black curve) exhibits sharp drops, indicating failure events (laboratory earthquakes). We wish to predict the time remaining before the next failure derived from the shear stress drops (red curve), using only the acoustic emission (dynamic strain) data (b). The dashed rectangle represents a moving time window; each window generates a single point on each feature curve below (e.g., variance, kurtosis, etc.). (c) The RF model predicts the time remaining before the next failure by averaging the predictions of 1000 decision trees for each time window. Each tree makes its prediction (white leaf node), following a series of decisions (colored nodes) based on features of the acoustic signal during the current window (see Supplementary Materials). (d) The RF prediction (blue line) on data it has never seen (testing data) with 90% confidence intervals (blue shaded region). The predictions agree remarkably well with the actual remaining times before failure (red curve). We emphasize that the testing data is entirely independent of the training data, and was not used to construct the model. Data from experiment number p2394.

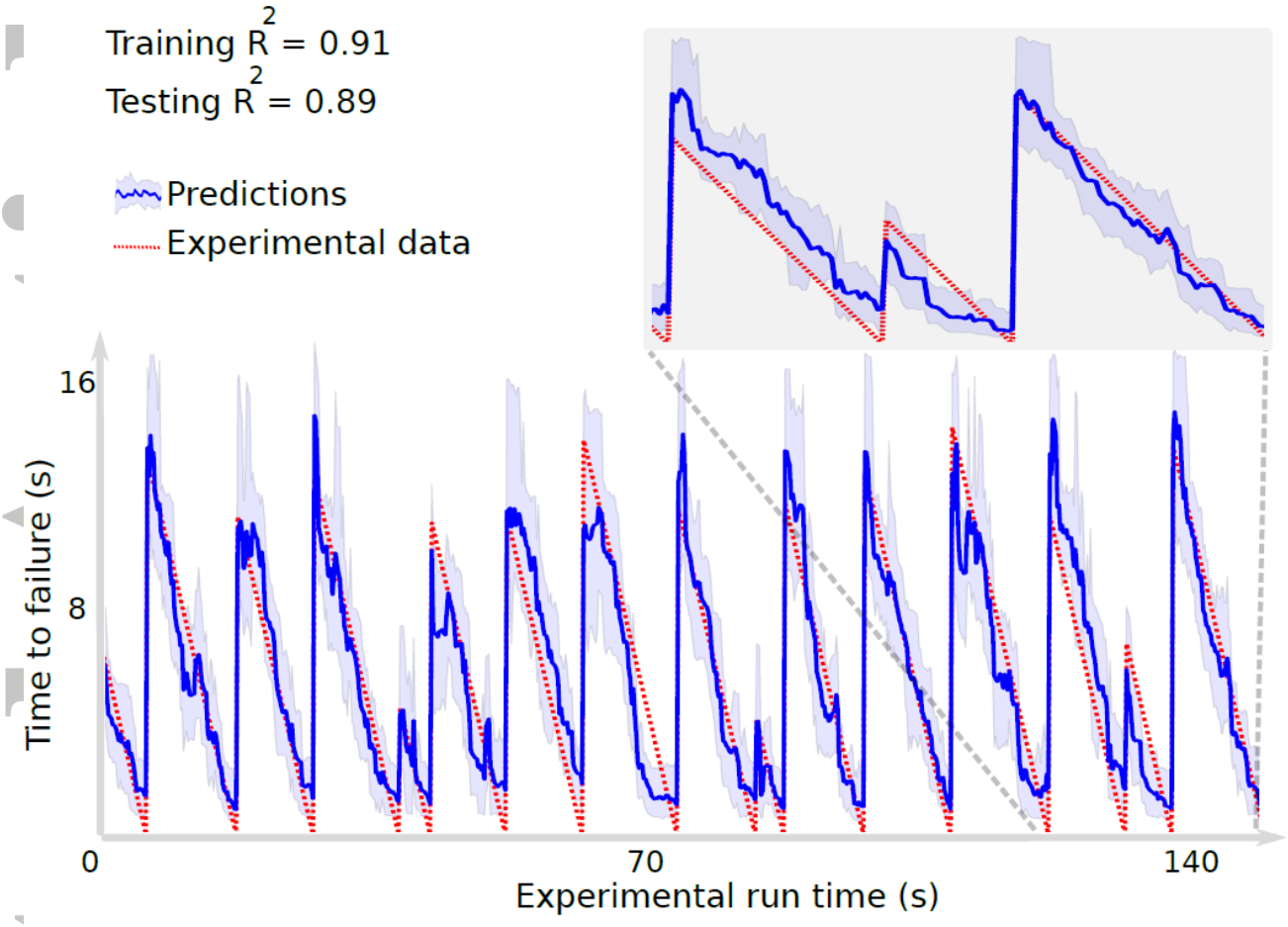

Figure 2. Time remaining before the next failure predicted by the Random Forest. As in Fig. 1a, the red lines show the actual time before failure (Y-axis) versus experimental run time (X-axis). The red dashed line shows the time remaining before the next failure (derived from the shear stress data), and the blue line shows the corresponding prediction of the RF regression model (derived exclusively from the 'instantaneous' acoustic data). The blue shaded region indicates the 5th and 95th percentiles of the forecast-that is, 90 percent of the trees that comprise the forest made a forecast within these bounds. The inset emphasizes predictions on aperiodic slip behavior. The RF does a remarkable job of forecasting slip times even with aperiodic data. The RF was trained on ≈150 seconds of data (≈10 slip events), and tested on the following ≈150 seconds, shown here. We stress that the predictions from each time are entirely independent of past and future history-each blue point is a 'now' prediction. The data points can be scrambled in time and the predictions remain the same. Data from experiment number p2394.

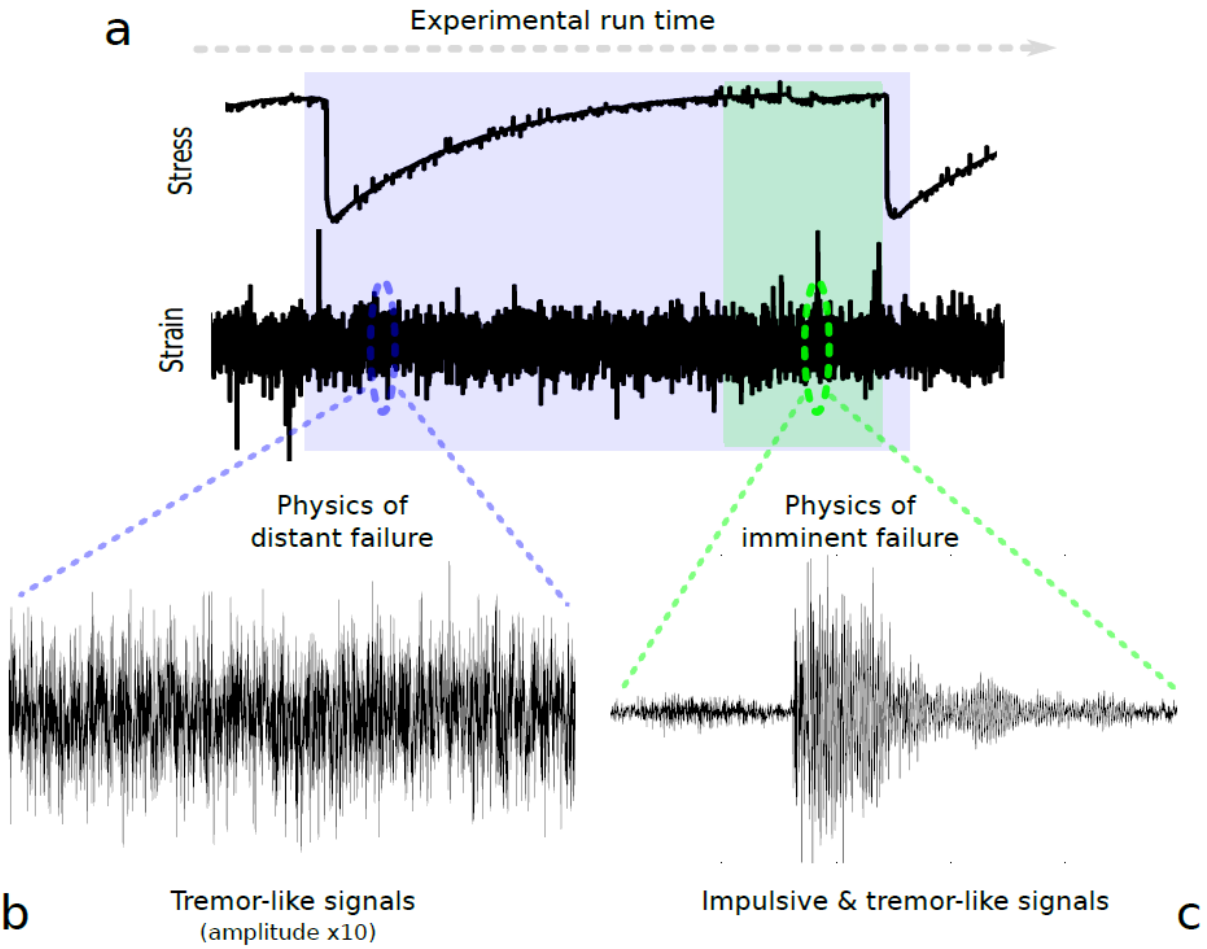

Figure 3. The physics of failure. The RF identifies two classes of signals and uses them to predict failure. (a) Shear stress and dynamic strain encompassing two failure events. (b) Zoom of dynamic strain when failure is in the distant future. This newly identified signal, termed 'laboratory tremor' offers precise predictive capability of the next failure time. (c) Zoom of a classic, impulsive acoustic emission observed in the critically stressed region just preceding failure (note vertical scale is different for two signals). Such signals are routinely identified preceding failure in the shear apparatus, in brittle failure in most materials and in some earthquakes. Data from experiment number p2394.